Intracellular complement C3/C3aR/STAT3 pathway inactivation attenuates retinal degeneration in mice

Shaojun Wang
Department of Opthalmology, Chinese PLA General Hospital https://orcid.org/0000-0002-5561-0952
Lu Du
Department of Opthamology, Chinese PLA General Hospital
Shunzong Yuan
Department of Lymphoma, Head and Neck Cancer, The Fifth Medical Center, Chinese PLA General Hospital
Guang-Hua Peng (ghp@zzu.edu.cn)
Zhengzhou University https://orcid.org/0000-0003-3813-6942

Research article

Keywords: complement C3, retinal pigment epithelium, retinal degeneration, membrane-attack-complex, apoptosis, age-related macular degeneration

Posted Date: December 22nd, 2020

DOI: https://doi.org/10.21203/rs.3.rs-131692/v1

Abstract

Background

Age-related macular degeneration (AMD) threatens vision in elderly people globally. Systemic complement C3 has been shown to be tightly associated with AMD. However, the mechanism of how local retinal complement C3 and downstream pathway mediated retinal degeneration is not entirely clear.

Methods

Wild-type, C3 knockout mice and mice treated with a C3aR inhibitor (SB290157), STAT3 inhibitor (SH-4-54), were exposed to sodium iodine ($NaIO_3$), respectively. C3 localization in degenerated retina was detected by using immunostaining. Retinal function was assessed by electroretinography, followed by histological analyses to assess RPE and photoreceptor cell degeneration. Retinal inflammation and mitochondrion were investigated through Real-time PCR, ELISA and RNA-Seq.

Results

We reported here that activation of complement was positively associated with retinal degeneration. Strikingly, intracellular C3 was activated in retinal pigment epithelial (RPE) cells, and subsequently promoted the formation of the membrane-attack complex (MAC), which contributed to apoptosis of RPE cells. Intracellular C3 deficiency or pharmalogical inhibition could rescue RPE cells from apoptosis. Moreover, genetic deletion of C3 or inhibition of C3aR/STAT3 results in alleviating immune response and rescue of photoreceptor cells under oxidative stress. Mechanistically, through RNA-Seq, we identified C3/C3aR/STAT3 pathway functionally mediated immune response and photoreceptor cell degeneration.

Conclusions

These results indicate that inhibition of the C3/C3aR/STAT3 pathway might be a new therapeutic intervention for AMD and other retinal degeneration diseases.

Background

Age-related macular degeneration (AMD) threatens vision of elderly people around the world, due to retinal pigment epithelium (RPE) and photoreceptor cells gradually degeneration [1]. Unfortunately, there are no effective treatments to reverse the RPE or photoreceptor cell degeneration in either neo-vascular ‘wet’ form or non-neo-vascular ‘dry’ form AMD [2]. Innate immune response, microglial cell activation and elevated levels of inflammatory cytokines contribute mainly to retinal degeneration [3–7]. The complement system is a part of innate immune defense system and plays a key role in retinal development and homeostasis [8].

Complement C3 is a central element in the complement system [9, 10], and C3 activation is the crucial step for triggering retinal injury [11, 12]. Studies have found elevated expression and deposition of C3 in pathological retina [13–16]. While majority studies focused on systemic C3 expression elevation during retinal degeneration, the role of local retinal C3 and how its downstream signal pathway involved in retinal cell degeneration remained incompletely understood. Intracellular C3 activation helps to sustain T cell homeostasis [17] and is responsible for damage to intestinal epithelial villi [18]. However, whether intracellular C3 activation exists in specific retinal cells during different stages of retinal degeneration is unknown. Two studies strongly indicate C3 in RPE and microglia cells [13, 19], while the mechanism of how C3 mediate retinal cells injury and microglia cell activation is not clear.

In this study, by employing the mouse AMD model established by sodium iodate ($NaIO_3$) stimulation, for the first time we demonstrated the important role of intracellular C3 activation in RPE degeneration, and identified C3/C3aR/STAT3 pathway mediating microglia activation and photoreceptor cell injury.

Methods

Animals

All studies were carried out on 8-week-old wild-type or C3-knockout C57BL/6J mice. The C3-knockout C57BL/6J mice were provided by Professor Yusen Zhou (State Key Laboratory of Pathogen and Biosecurity, Beijing Institute of Microbiology and Epidemiology, Beijing 100071, China). All animals were housed in a pathogen-free, temperature-controlled animal facility with 12/12-h light/dark cycles and fed with standard food and water *ad libitum*. All of the animal protocol was approved by the Institutional Animal Care and Use Committee of the General Hospital of the Chinese People's Liberation Army and Zhengzhou University in accordance with the National Institutes of Health Guidelines for the Care and Use of Laboratory Animals. All efforts were made to reduce the number of animals used and minimize the suffering caused by experimental procedures.

Treatment with sodium iodate and tissue collection

We selected sodium iodate ($NaIO_3$) (Sigma-Aldrich, USA) for the retinal degeneration model according to a previous publication [20]. Briefly, mice in experimental groups were administered a single dose of 35 mg/kg $NaIO_3$ dissolved in saline via femoral vein injection. The mice in the control group were administered the equivalent volume of saline. The $NaIO_3$-treated and control mice (n = 6 per group) were examined by electroretinography (ERG) and multifocal electroretinography (mfERG) and then eyeballs were collected from 1 to 28 days by enucleating the mice and immersing the eyeballs in 4% paraformaldehyde in 0.1 M phosphate buffer.

Histology and Immunofluorescence

After fixation for 24 hours, the anterior section of the eyes was dissected and the remaining eye cup was dehydrated, then embedded in paraffin wax. Sections (at 4 μm) were cut on a microtome (Shandon

AS325; Thermo Scientific, USA). All histologic analyses for outer nuclear layer (ONL) thickness used retinal sections cut along the parasagittal plane (super inferior), as described previously [21]. These sections also included the ocular nerve head, in order to maintain regional consistency between replicates and groups. H&E staining was performed, and images were captured with a microscope (Olympus, Japan). For each section, 18 measurements spaced 200-μm apart were made to analyze ONL damage. Three measurements were made per sample and averaged.

For immunostaining, sections were dewaxed, subjected to antigen-retrieval and blocked with 10% goat serum (Sigma-Aldrich Corp.) in 0.2% Triton X-100 (Sigma-Aldrich Corp.) phosphate-buffered saline for 1 hour and incubated with primary antibodies in a humidity chamber overnight at 40^0 C. Primary antibodies were listed as follows: anti-Complement C3, 1:300; anti-Iba1, 1:300; anti-rhodopsin, 1:600; anti-RPE65, 1:300; anti- C_{6b-9}, 1:300; anti-ATP5A, 1:300; anti-C3aR, 1:300, anti-pSTAT3, 1:300. All antibodies were from Abcam. After washing and incubation for 1 hour at room temperature with secondary antibodies, sections were counterstained with ProLong Gold with DAPI (Invitrogen) to reveal cell nuclei. Images were obtained using an Olympus FV3000 confocal microscope and were taken at the corresponding histologically defined areas of the sections. All images in each individual experiment were acquired with a fixed detection gain. Images were processed and semi-quantified by using Image J.

ERG and mfERG

ERG was performed using the Espion E3 console in conjunction with the ColorDome (Diagnosys LLC). The ERG experiments were carried out on C57B6 wild-type or C3 knockout mice at 1-week post-injection. In brief, the mice were dark-adapted the night before the recordings were performed. The animals were anesthetized by a subcutaneous injection of xylazine (15 mg/kg) and ketamine (110 mg/kg). The animals' pupils were dilated using 1% tropicamide. The animals were positioned on a water warming pad to prevent hypothermia. In each animal, only the right eye was examined. Active gold electrodes were placed on the right eye cornea as the recording electrodes. The reference and ground electrodes were placed subcutaneously in the mid-frontal areas of the head and tail, respectively. We applied light stimulation at densities of 0.5 log ($cd{\cdot}s/m^2$). The amplitudes of a- and b-waves were recorded and processed using a RETI-Port device (Roland Consult). All procedures were performed in a dark room under a dim red safety light.

For mfERG, the animals were positioned 10cm in front of the stimulating screen. An array of equally sized hexagons was projected on to the retina. The stimuli were generated by a projector with a refresh rate of 60 Hz. In the m-sequence, the luminance of the hexagons was either 150 cd/m^2 (corresponding to 2.5 cd s/m^2 in a single frame) or less than 1 cd/m^2. The m-exponent was 9, resulting in 511 m-sequences for each cycle. Eight cycles were averaged for a final result.

TUNEL staining

TdT-UTP nick end labeling (TUNEL) assay was performed with the one step TUNEL kit according to the manufacturer's instructions (Beyond, Shanghai). Paraffin sections and cells grown in 24-well plates treated with $NaIO_3$ was fixed. Briefly, the cells were permeabilized with 0.1% Triton X-100 for 10 min at room temperature. followed by TUNEL for 1 h at 37° C. The FITC-labeled TUNEL-positive cells were imaged under a fluorescent microscope by using 488 nm excitation and 530 nm emission. The cells with green fluorescence were defined as apoptotic cells.

Apoptosis and mitochondrial membrane potential assays

Early apoptosis was investigated by confocal microscopy using the mitochondrial membrane potential apoptosis kit with Alexa Fluor 488 Annexin V and Mito Tracker Red (Beyond, Shanghai). Cells were seeded in the confocal chamber at a density of 200,000 cells/well and incubated for 36 hours. After $NaIO_3$ stimulation pretreated with or without C3 (10μM, MCE, USA), E64d (10μM, Beyond, Shanghai), cell medium was removed. Alexa Fluor 488 Annexin V and Mito Tracker Red dye was added to the culture medium following the manufacturer's protocols and incubated for 30 min at 37 ^{0}C. The cells were then analyzed by using laser confocal microscopy (Olympus, Japan).

Primary RPE cell culture

C57BL/6J wild-type or C3 knockout mouse primary RPE cell culture was performed as previously described [22]. Briefly, eyes were removed from 2-week-old C57BL/6J mice after deep anesthesia, and the RPE layer was collected and digested by trypsin, centrifuged, suspended in culture medium, seeded in 12 mm polyester membrane inserts. By 3 weeks of culture, the cells were stimulated with $NaIO_3$ (10mM), and in the experimental group C3, E64d were added respectively.

Application of drugs

C3aR antagonist (SB290157) and STAT3 inhibitor (SH-4-54) was purchased from Selleck (S8931 and S7337) and solved under manufacturer's instructions. Mice were pretreated with SB290157 (10mg/kg) or SH-4-54 3 days before $NaIO_3$ injection and then three times a week via i. p. injection for 1week. After ERG assay, mice were sacrificed and retinal tissue were collected for immunoassaying and real-time PCR assay.

RNA extraction and real-time PCR

Total RNA was extracted and real-time PCR assay was conducted as previously reported [23]. Primer sequences are listed as below:

Gene	F	R
mC1qa	CAAGGACTGAAGGGCGTGAA	CAAGCGTCATTGGGTTCTGC
mC2	CTCATCCGCGTTTACTCCAT	TGTTCTGTTCGATGCTCAGG
mC3	GAAGTACCTCATGTGGGGCC	CAGTTGGGACAACCATAAACC
mC3aR	GGAAGCTGTGATGTCCTGG	CACACATCTGTACTCATATTGT
mCfb	GAGGATGGGCACAGCCCAG	GACCATATCGTGGCCTCACC
mCfd	GCAGAGAGCAACCGCAGG	CAGGATGTCATGTTACCATTTG
mCfh	CTTACATGCATGTGTAATACCA	TTATACACAAGTGGGATAATTGA
mCfi	CCATTGATGCCTGCAAAGGA	CAGACATTGTGTTGAGAAACAA
mCD68	ACTGGTGTAGCCTAGCTGGT	CCTTGGGCTATAAGCGGTCC
mTNFα	CCCTCACACTCAGATCATCTTCT	GCTACGACGTGGGCTACAG
mIL1β	GCAACTGTTCCTGAACTCAACT	ATCTTTTGGGGTCCGTCAACT
mIL6	TAGTCCTTCCTACCCCAATTTCC	TTGGTCCTTAGCCACTCCTTC
mNfe2l2	GCCTTACTCTCCCAGTGAATAC	CCCAAATGGTGCCTAAGA
mStat3	CAGAAAGTGTCCTACAAGGGCG	CGTTGTTAGACTCCTCCATGTTC
mSOD2	CAGGATGCCGCTCCGTTAT	TGAGGTTTACACGACCGCTG
mGCLM	TCAACCCAGATTTGGTCAGGGAGT	TCCAGCTGTGCAACTCCAAGGA
mNQO1	TGAAGAAGAAAGGATGGGAGG	AGGGGGAACTGGAATATCAC
mPGC-1α	TGCTGTGTGTCAGAGTGGATTGGA	ACCAACCAGAGCAGCACACTCTAT
mNRF-1	TCTGAGACGCTGCTTTCAGTCCTT	TGGGCTTCTATGGTAGCCATGTGT
mCOXII	ACCTGGTGAACTACGACTGCTAGA	TGCTTGATTTAGTCGGCCGAT
mTFAM	TGGCAGTCCATAGGCACCGTATT	ACAGACAAGACTGATAGACGAGGG
mβ–actin1	CGAGAAGATGACCCAGATCATGTT	CCTCGTAGATGGGCACAGTGT

RNA-seq and data analysis

First, we collected retina tissue from normal control and 7-days after $NaIO_3$ induction of wild-type mice, then the total RNA was extracted. The RNA-seq analysis was performed using Illumina NovaSeq6000 with the depth of 60 million pairs of reads per sample. Three mice per group (total of 6 mice) were analyzed. Raw reads were first aligned to the Mus musculus genome (UCSC mm10) using Hisat2 with default parameters. Then, htseq-count function of HTSeq was used to accumulate the number of aligned reads that fall under the exons of the gene (union of all the exons of the gene) to present the expression

of each gene. We identified differential gene by using the DESeq2 package in the R environment [24]. Finally, Gene Ontology (GO) analysis was performed.

Statistical Analysis

Statistical analysis of the two groups was performed using 2-tailed paired Student's t-tests assuming equal variance. Results were expressed as Mean±SEM deviation. Differences were considered significant at $P < 0.05$.

Results

Complement activation following $NaIO_3$ stimulation

We administered $NaIO_3$ to 8-wk-old wild-type mice to induce retinal degeneration. From the landscape image of the retinal sagittal section collected from different time after $NaIO_3$ induction, the thickness of outer nuclear layer (ONL) was significantly reduced in wild-type mice from day 7 (Figure 1 A, B). By employing real-time PCR, we measured complement C1qa, C2, C3, Cfd, Cfb, Cfh, Cfi mRNA level in mice at control, day 1 and day 7 after $NaIO_3$ treatment (Figure 1 C-I). Complement C3 and Cfi were elevated as early as day 1 after $NaIO_3$ application compared with control, and further elevated at day 7 (Figure 1 E, I). Complement C1qa and C2 had no obvious change at day 1, but were significantly upregulated at day 7 (Figure 1 C, D). Complement Cfd, Cfb and Cfh were downregulated as early as day 1 after $NaIO_3$ application, while Cfd and Cfb were upregulated at day 7 (Figure 1 F-H). These findings suggested activation of local retinal complement pathway began at day 1 during retinal degeneration.

Intracellular C3 activation in RPE after $NaIO_3$ stimulation

Fluorescent immunostaining and confocal laser scanning image showed robust complement C3 intracellular distribution of RPE cells at day 1 (Figure 2 A). In addition, double fluorescent immunostaining of RPE65 and C3 displayed down-regulation of RPE65 and up-regulation of C3 in RPE cells day 1. These results indicated intracellular C3 accumulation correlated with RPE injury (Figure 2 B). TUNEL staining confirmed that RPE apoptosis, which induced by $NaIO_3$ at day 1, was obviously reduced by genetic deletion of C3 (Figure 2 C, D). To further investigate the direct relationship between C3 expression and RPE apoptosis resulting from $NaIO_3$ stimulation, we isolated RPE cells and added 10mM $NaIO_3$ to an *in vitro* culture system. The results demonstrated that as early as 4 hours, C3 staining was unambiguously observed in RPE cells (Figure 2 E). Subsequently, apoptosis was observed at 24 hours (Figure 2 F, G). In contrast, no C3 expression or apoptosis were detected in C3-deficient RPE cells 24 hours after $NaIO_3$ stimulation *in vitro* (Figure 2 E, F).

To better identify RPE apoptosis induced by $NaIO_3$ was not caused by extracellular C3, we injected C3 into C3-deficient mice after $NaIO_3$ injection by means of the tail vein every day. The results showed exogenous C3 caused no obvious damage to ONL in C3-deficient mice day 7 after $NaIO_3$ treatment (Figure S1). In

addition, there was no apoptosis in wild-type RPE cells after different doses of C3 in the *in vitro* culture system. We also detected no apoptosis in C3-deficient RPE cells *in vitro* under C3 and $NaIO_3$ stimulation (Figure S1). These results indicated RPE apoptosis induced by $NaIO_3$ might be dependent on endogenous C3.

Intracellular C3 activation contributed to RPE injury

C3 and MAC-mediated apoptosis play an important role in retinal injury or neuro-degeneration [25, 26]. Intracellular C3 accumulation has been shown to cause cell apoptosis, although the mechanism was unclear [18] . As C_{6b-9} is the downstream pathway of C3 activation. To investigate the potential mechanism of RPE-cell apoptosis led by C3 intracellular accumulation, we detected the components of MAC in RPE cells after $NaIO_3$ stimulation. C_{6b-9} could be detected in wild-type RPE cells day 1 after $NaIO_3$ stimulation *in vivo*, but no C_{6b-9} was detected in C3-deficient RPE cells (Figure 3 A). Just as with *in vivo* findings, C_{6b-9} could be detected in wild-type RPE cells 4 hours after $NaIO_3$ stimulation *in vitro*, but no C_{6b-9} was detected till 24 hours in C3-deficient RPE cells (Figure 3 B). Moreover, multiple-immunostaining showed the reduction of mitochondrion quantity in wild-type RPE cells day 1 after $NaIO_3$ stimulation *in vivo* and *in vitro,* knockout of C3 could reserve mitochondrial quantity. We also observed up-regulation of PGC-1α, NRF1 and TFAM mRNA levels in normal C3-deficient retina. By real-time PCR assay, mRNA levels of COX-Ⅳ, PGC-1α, NRF1, TFAM, Nre2l2, SOD2, NQO1 and GCLM are higher in C3-deficient retina than in wild-type after $NaIO_3$ stimulation. These results indicate knockout of C3 could protect retina damage from oxidative stress by enhancing anti-oxidative stress involved signal pathway.

Inhibition of intracellular C3 activation reducing RPE apoptosis

Normally, no apoptosis or mitochondrial malfunction were observed in wild-type RPE cells cultured *in vitro*, which were detected by Annexin V and Mito-tracker staining. After applying $NaIO_3$ to the *in vitro* culture system, wild-type RPE cells appeared to show early apoptosis and mitochondrial malfunction within 2 hours; but no apoptosis was detected in C3-deficient RPE cells at the same time point (Figure 4 A). Intracellular C3 activation could be blocked by the specific cathepsin inhibitor E64, which has been illustrated in T cells [17]. Indeed, we observed significantly decreased apoptosis and mitochondrial malfunction in wild-type RPE cells exposed to E64 1 hour prior to $NaIO_3$ stimulation, but the inhibition effect was still less than that achieved by C3-deficiency (Fig. 4 A). We also observed significantly decreased C3 and $C6_{b-9}$ in wild-type RPE cells exposed to E64 1 hour prior to $NaIO_3$ stimulation *in vitro* (Fig. 4 B). TUNEL staining showed decreasing RPE apoptosis after $NaIO_3$ stimulation pretreated with E64 *in vivo* (Figure 4 C). Multiple fluorescent immunostainings demonstrated normalized RPE65 expression and reduced C3 and MAC after $NaIO_3$ stimulation pretreated with E64 (Figure 4 D). Real-time PCR assay of SOD2, NQO1 and GCLM level revealed E64 pre-treatment could enhance the anti-oxidative stress response in wild-type RPE cell.

Knockout of C3 alleviate microglia activation and inflammatory response

Immune response plays an important role in photoreceptor cell degeneration [27]. To investigate the role of C3 in immune regulation, immunostaining using anti-GFAP and anti-Iba1 antibodies revealed remarkable increase in GFAP and Iba1 fluorescent at day 7 retinas after $NaIO_3$ stimulation (Figure 5 A). Strikingly, C3-deficient nearly completely normalized the GFAP and Iba1 immunoreactivity (Figure 5 A, B). To discover the retinal locus of C3 at day 7 after $NaIO_3$ induction, we performed multiple fluorescent immunostainings with anti-GFAP, anti-Iba1, anti-CD68 and anti-C3 antibodies. C3 colocalized predominantly with $Iba1^+$ cells, indicating microglia activation during photoreceptor cell degeneration. Microglia and Muller glia activation is associated with increased production of pro-inflammatory cytokines including TNFα, IL6, and IL1α. All three cytokines were elevated in retina tissues at day 7 after $NaIO_3$ stimulation, where C3-deficient resulted in significant dampening of these cytokine levels (Figure 5 C, D). These results supported that C3 and its downstream signal pathway regulated microglia and Muller glia cell reactivity and the production of proinflammatory cytokines in $NaIO_3$ induced retinal degeneration.

Knockout of C3 reduced photoreceptor cell apoptosis

The above studies demonstrated the prominent role of C3 in RPE injury and immune regulation. We next sought to assess the role of C3 in photoreceptor cell degeneration. HE staining revealed no difference in the neural retinal structure between wild-type and C3-deficient normal mice. We observed a significant reduction in ONL thickness at day 7 after $NaIO_3$ induction compared to controls. In contrast, ONL thickness was not significantly changed between C3-deficient mice at day 7 compared to controls (Figure 6 A, B). Remarkably, electroretinogram (ERG) a and b wave significantly diminished in wild-type mice at day 7 after $NaIO_3$ induction and a significant rescue in C3-deficient mice (Figure S2). As rhodopsin is a key protein for phototransduction, we analyzed the expression of rhodopsin and found it was significantly down-regulated in wild-type mice compared with C3-deficient mice after $NaIO_3$ injection (Figure 6 C, D). Furthermore, TUNEL staining showed apoptosis of photoreceptor cell was significantly reduced in C3 knockout group at day 7 (Figure 6 E, F). These results indicated that C3 played an important role in $NaIO_3$-induced retinal photoreceptor cell degeneration and inactivation of C3 could reserve retinal function.

RNA-Seq identified C3aR/STAT3 signal involved in retinal degeneration

To further investigate the mechanisms involving complement C3 pathway to photoreceptor degeneration, we compared the mRNA in day 7 versus controls retina using RNA-seq analysis. The bioinformatics analysis has identified the top changed genes between control and $NaIO_3$ induction day 7 retinas (DE; fold-change >2.0, $p < 0.05$). DEGs has shown the down-regulation of photo-transduction genes, such as Arrestin3, Rhodopsin, Rgr and etc; the C3, C3aR and STAT3 mRNA level up-regulated obviously (Figure 7A). Gene Ontology (GO) has shown the up-regulated signal pathway, the STAT cascade included; the signal pathway involved phototransduction and visual perception were down-regulated (Figure 7 B, C). In pathological conditions, C3 could be spliced into C3b and C3a, C3a binds to its receptor C3aR. Enhanced expression of C3aR and activation of subsequent downstream signal may amplify its downstream

pathological effect. Previous study has indicated that C3aR regulates the expression of STAT3 and mediated inflammatory [28], which is not clear in retina. Then, real-time PCR and immunostaining result confirmed the elevation of C3aR and pSTAT3 in mRNA and protein levels day 7 after $NaIO_3$ induction (Figure 7 D, E). Knockout of C3 also normalized the up-regulation of C3aR and pSTAT3 (data not shown). Our findings suggested that enhanced expression of C3aR/pSTAT3 might contribute to microglia activation, inflammatory response and photoreceptor degeneration after $NaIO_3$ induction.

Inhibition of C3aR/pSTAT3 mitigates photoreceptor cell degeneration

To gain a deeper understanding of C3/C3aR/STAT3 signal in photoreceptor degeneration, we inactivated C3aR or STAT3 pharmacologically. Wild-type mice were pretreated with C3aR antagonist SB290157 3 days before treated with $NaIO_3$, and then intra-peritoneal injected every other day. $TUNEL^+$ photoreceptor cell was obviously reduced compared with the non-SB290157 control group at day 7 of $NaIO_3$ induction (Figure 8 A). Multiple fluorescent immunostainings found C3aR antagonist obviously down-regulated GFAP expression and microglial cell activation (Figure 8 B, C). Real-time PCR analysis revealed the down-regulation of TNFα mRNA level after application of SB290157 (Figure 8 D). Both the mRNA and phosphonate-protein levels of STAT3 were observed down-regulated with SB290157 compared only $NaIO_3$ induction group (Figure 8 E, F). The activation of the STAT pathway involves in immune response [28, 29]. To confirm the role of STAT3 activation in retinal degeneration, wild-type mice were pretreated with STAT3 inhibitor SH-4-54 3-days before $NaIO_3$ application. Apoptosis ratio of photoreceptor cell was alleviated and the ERG a and b waves have been partially preserved, which indicated the retinal protection effect of STAT3 inhibitor. Taken together, these day 7 results established a novel signaling pathway (C3/C3aR/STAT3) linking microglia activation and photoreceptor cell degeneration.

Discussion

RPE cell injury and subsequent photoreceptor cell death are the main cause of AMD and many other retinal degeneration diseases, but the mechanism remains incompletely addressed so far. Understanding the mechanism will help to develop potential treatments for RPE and photoreceptor cell injury-related diseases. In this study, we not only found intracellular C3 deficiency played a vital role in preventing RPE apoptosis, but also identified the C3/C3aR/STAT3 pathway play important role in mediating immune response and photoreceptor cell apoptosis under oxidative stress, which might be helpful for treating retinal degeneration diseases.

AMD is classified into two forms, a non-neovascular or ‘dry’ form and a neovascular or ‘wet’ form. Treatment using anti-vascular endothelial cell growth factor is available for wet AMD [30], but no effective prevention or treatment is available for the ‘dry’ form. While no animal model fully recapitulates the pathologic features found in ‘dry’ AMD, $NaIO_3$-induced RPE apoptosis is considered as the best model for this disease [31, 32]. It has been widely used for the evaluation of preclinical efficacy of novel therapeutics for geographic atrophy, one of the major features in ‘dry’ AMD. One previous study has

shown that irreversible photoreceptor and RPE cell damage in mice treated with $NaIO_3$ is related to macrophage accumulation [33]. There is a relationship between oxidative stress and complement activation in AMD models [34].

Complement and microglial cells mediate neural-cell damage in many retinal degeneration diseases, such as AMD, Stargardt disease and glaucoma [19, 25, 35]. As the critical component of the complement system, how C3 acts in RPE and photoreceptor cells death is not clear. In this study, we observed the activation of microglial cells 7 days after $NaIO_3$ injection, and the co-localization of C3 and microglial cells was consistent with previous reports. Unexpectedly, we found early C3 accumulation in apoptotic RPE cells. Traditionally, C3 is secreted by hepatocytes. However, recently two studies have identified functional C3 expression in non-hepatic cells, such as lymphocytes and intestinal epithelial cells [17, 18]; this inspired us to explore the role of intracellular C3 in RPE injury induced by $NaIO_3$. Simultaneously, through single cell RNA-seq study, Pauly et al. firstly explored the character of complement components in specific retinal cell types in normal and pathological condition, their results strongly indicate a local retinal complement activated possibly independent of the systemic components typically produced by the liver during retinal degeneration [36]. Through *in vivo* and *in vitro* experiments, for the first time, we have found that $NaIO_3$-induced RPE apoptosis and mitochondrial malfunction were dependent on intracellular endogenous C3, which was partially mediated by cathepsin. However, in our future work, we need fully demonstrate the role of complement activation on mitochondrion pathological change.

Another important finding in our study was that MAC formation might be the main reason for RPE apoptosis and mitochondrial malfunction after intracellular C3 activation. However, the exact mechanism here is to be explored further. We assume that the activated C3 might be released into the extracellular matrix after RPE apoptosis and subsequently induces the migration, aggregation and activation of microglial cells. This might explain why microglial cells appear later than RPE apoptosis in the retina after $NaIO_3$ stimulation *in vivo*.

Mechanistically, we identified STAT3 as a downstream gene of C3/C3aR pathway during photoreceptor cell degeneration. Our RNA-seq analysis revealed a significant activation of C3/C3aR/STAT cascade in $NaIO_3$ induced retinal degeneration model. Strikingly, genetic deletion of C3 or pharmacological inhibition of C3aR or STAT3 could obviously prevent photoreceptor loss and reserve retinal function. Moreover, the immune response, such as the pro-inflammatory cytokines release and microglial infiltration and Muller glial reactivity was suppressed after blocking C3/C3aR/STAT3 pathway.

Conclusions

Taken together, our current study demonstrates that RPE injury induced by $NaIO_3$ was endogenous C3 dependent. And activation of C3/C3aR/STAT3 pathway play important role in mediating microglia activation and photoreceptor cell degeneration. Therefore, inhibition of intracellular C3 and normalized C3/C3aR/STAT3 pathway could be helpful in preventing AMD or other retinal degeneration disease.

Abbreviations

AMD: Age-related macular degeneration; ARVO: Association for Research in Vision and Ophthalmology; C1qa: Complement component 1q subcomponent alpha; C2: Complement component 2; C3: Complement component 3; C3a: Complement component 3 subcomponent alpha; C3aR: Complement component 3 subcomponent alpha receptor; C3b: Complement component 3 subcomponent beta; Cfb: Complement factor B; Cfd: Complement factor D; Cfh: Complement factor H; Cfi: Complement factor I; CD68: Cluster of differentiation 68; COXII: Cytochrome oxidase subunit II; DEGs: Different expression genes; ERG: Electroretinographic recording; FBS: Fetal bovine serum; GCLM: Glutamate cysteine ligase, modifier subunit; GFAP: Glial fibrillary acidic protein; GO: Gene Ontology; Iba-1: Ionized calcium binding adaptor molecule 1; IL-1β: Interleukin 1β; IL-6: Interleukin 6; MAC: Membrane-attack complex; mRNA: Messenger RNA; NaIO3: Sodium iodate; Nfe2l2: Nuclear factor erythroid 2-related factor 2; NQO1: NAD(P)H quinone dehydrogenase 1; NRF-1: Nuclear respiratory factor 1; ONL: outer nuclear layer; PBS: Phosphate-buffered saline; PCR: Polymerase chain reaction; PGC-1α: Peroxisome proliferator-activated receptor-γ coactlvator-1; RPE: Retinal pigment epithelial; SEM: Standard error of mean; SOD2: Superoxide Dismutase-2; STAT3: Signal Transducers and Activators of Transcription; TFAM: Mitochondrial transcription factor A; TNFα: Tumor necrosis factorα; TUNEL: TdT-UTP nick end labeling; WT: Wild-type.

Declarations

Ethics approval and consent to participate

All experiments were conducted in accordance with the ARVO Statement

for Use of Animals in Ophthalmic and Vision Research, and had approval

from the Institutional Animal Care and Use Committee of the General Hospital of the Chinese People's Liberation Army and Zhengzhou University in accordance with the National Institutes of Health Guidelines for the Care and Use of Laboratory Animals. All efforts were made to reduce the number of animals used and minimize the suffering caused by experimental procedures.

Consent for publication

All authors consent for the publication of this study.

Availability of supporting data

All data generated or analyzed during this study are included in this published article.

Competing interests

The authors declare that they have no competing interests.

Funding

This work was supported by the National Key Research and Development program (2018YFA0107303 to Guang-Hua Peng), National Natural Science Foundation of China (NSFC 81501090 to Shaojun Wang), Distinguished Professor Initiation Fund, Zhengzhou University (No. 32310180 to Guang-Hua Peng), China Postdoctoral Research Fund (Issue 2017M613396 to Shaojun Wang).

Author contributions

Shaojun Wang and Lu Du conceived and designed the study. Shaojun Wang and Lu Du performed animal model preparation and RPE culture, and immunohistochemistry. Shaojun Wang, Lu Du and Shunzong Yuan analyzed data and wrote the manuscript. Guang-Hua Peng provided support and supervised the project. All authors read and approved the final manuscript.

Acknowledgements

We thank Dr Brian Eyden (Manchester, United Kingdom) for his kind linguistic revision of the manuscript. The C3-knockout C57BL/6J mice were a kind gift from ceased Professor Yusen Zhou (State Key Laboratory of Pathogen and Biosecurity, Beijing Institute of Microbiology and Epidemiology, Beijing 100071, China).

Author' information

1. Laboratory of Visual Cell Differentiation and Regulation, Basic Medical College, Zhengzhou University, Zhengzhou, Henan Province, 450001, China. 2. Department of Ophthalmology, Chinese PLA General Hospital, Beijing 100039, China. 3. Department of Lymphoma, Head and Neck Cancer, The Fifth Medical Center, Chinese PLA General Hospital (Former 307th Hospital of the PLA), Beijing 100071, China. 4. Department of Pathophysiology, Basic Medical College, Zhengzhou University, Zhengzhou, Henan Province 450001, China.

References

1. Handa JT, Bowes Rickman C, Dick AD, Gorin MB, Miller JW, Toth CA, Ueffing M, Zarbin M, Farrer LA: **A systems biology approach towards understanding and treating non-neovascular age-related macular degeneration.** *Nature Communications* 2019, **10:**3347.
2. Wong WL, Su X, Li X, Cheung CM, Klein R, Cheng CY, Wong TY: **Global prevalence of age-related macular degeneration and disease burden projection for 2020 and 2040: a systematic review and meta-analysis.** *The Lancet Global health* 2014, **2:**e106-116.
3. Ambati J, Fowler BJ: **Mechanisms of age-related macular degeneration.** *Neuron* 2012, **75:**26-39.
4. Orozco LD, Chen HH, Cox C, Katschke KJ, Jr., Arceo R, Espiritu C, Caplazi P, Nghiem SS, Chen YJ, Modrusan Z, et al: **Integration of eQTL and a Single-Cell Atlas in the Human Eye Identifies Causal Genes for Age-Related Macular Degeneration.** *Cell Rep* 2020, **30:**1246-1259.e1246.

5. Menon M, Mohammadi S, Davila-Velderrain J, Goods BA, Cadwell TD, Xing Y, Stemmer-Rachamimov A, Shalek AK, Love JC, Kellis M, Hafler BP: **Single-cell transcriptomic atlas of the human retina identifies cell types associated with age-related macular degeneration.** *Nat Commun* 2019, **10:**4902.
6. Voigt AP, Mulfaul K, Mullin NK, Flamme-Wiese MJ, Giacalone JC, Stone EM, Tucker BA, Scheetz TE, Mullins RF: **Single-cell transcriptomics of the human retinal pigment epithelium and choroid in health and macular degeneration.** *Proc Natl Acad Sci U S A* 2019, **116:**24100-24107.
7. Mulfaul K, Ozaki E, Fernando N, Brennan K, Chirco KR, Connolly E, Greene C, Maminishkis A, Salomon RG, Linetsky M, et al: **Toll-like Receptor 2 Facilitates Oxidative Damage-Induced Retinal Degeneration.** *Cell Rep* 2020, **30:**2209-2224.e2205.
8. Akhtar-Schafer I, Wang L, Krohne TU, Xu H, Langmann T: **Modulation of three key innate immune pathways for the most common retinal degenerative diseases.** *EMBO molecular medicine* 2018, **10**.
9. Ricklin D, Reis ES, Mastellos DC, Gros P, Lambris JD: **Complement component C3 - The "Swiss Army Knife" of innate immunity and host defense.** *Immunological reviews* 2016, **274:**33-58.
10. Liszewski MK, Java A, Schramm EC, Atkinson JP: **Complement Dysregulation and Disease: Insights from Contemporary Genetics.** *Annual review of pathology* 2017, **12:**25-52.
11. van Lookeren Campagne M, Strauss EC, Yaspan BL: **Age-related macular degeneration: Complement in action.** *Immunobiology* 2016, **221:**733-739.
12. Mohlin C, Sandholm K, Ekdahl KN, Nilsson B: **The link between morphology and complement in ocular disease.** *Molecular immunology* 2017, **89:**84-99.
13. Linetsky M, Bondelid KS, Losovskiy S, Gabyak V, Rullo MJ, Stiadle TI, Munjapara V, Saxena P, Ma D, Cheng YS, et al: **4-Hydroxy-7-oxo-5-heptenoic Acid Lactone Is a Potent Inducer of the Complement Pathway in Human Retinal Pigmented Epithelial Cells.** *Chemical research in toxicology* 2018, **31:**666-679.
14. Stephan AH, Barres BA, Stevens B: **The complement system: an unexpected role in synaptic pruning during development and disease.** *Annual review of neuroscience* 2012, **35:**369-389.
15. Chi ZL, Yoshida T, Lambris JD, Iwata T: **Suppression of drusen formation by compstatin, a peptide inhibitor of complement C3 activation, on cynomolgus monkey with early-onset macular degeneration.** *Adv Exp Med Biol* 2010, **703:**127-135.
16. Ramos de Carvalho JE, Klaassen I, Vogels IM, Schipper-Krom S, van Noorden CJ, Reits E, Gorgels TG, Bergen AA, Schlingemann RO: **Complement factor C3a alters proteasome function in human RPE cells and in an animal model of age-related RPE degeneration.** *Invest Ophthalmol Vis Sci* 2013, **54:**6489-6501.
17. Liszewski MK, Kolev M, Le Friec G, Leung M, Bertram PG, Fara AF, Subias M, Pickering MC, Drouet C, Meri S, et al: **Intracellular complement activation sustains T cell homeostasis and mediates effector differentiation.** *Immunity* 2013, **39:**1143-1157.
18. Satyam A, Kannan L, Matsumoto N, Geha M, Lapchak PH, Bosse R, Shi GP, Dalle Lucca JJ, Tsokos MG, Tsokos GC: **Intracellular Activation of Complement 3 Is Responsible for Intestinal Tissue Damage during Mesenteric Ischemia.** *Journal of immunology* 2017, **198:**788-797.

19. Natoli R, Fernando N, Jiao H, Racic T, Madigan M, Barnett NL, Chu-Tan JA, Valter K, Provis J, Rutar M: **Retinal Macrophages Synthesize C3 and Activate Complement in AMD and in Models of Focal Retinal Degeneration.** *Invest Ophthalmol Vis Sci* 2017, **58:**2977-2990.
20. Xiao J, Yao J, Jia L, Lin C, Zacks DN: **Protective Effect of Met12, a Small Peptide Inhibitor of Fas, on the Retinal Pigment Epithelium and Photoreceptor After Sodium Iodate Injury.** *Invest Ophthalmol Vis Sci* 2017, **58:**1801-1810.
21. Wang J, Iacovelli J, Spencer C, Saint-Geniez M: **Direct effect of sodium iodate on neurosensory retina.** *Invest Ophthalmol Vis Sci* 2014, **55:**1941-1953.
22. Shang P, Stepicheva NA, Hose S, Zigler JS, Jr., Sinha D: **Primary Cell Cultures from the Mouse Retinal Pigment Epithelium.** *J Vis Exp* 2018.
23. Wang S, Du L, Peng GH: **Optogenetic stimulation inhibits the self-renewal of mouse embryonic stem cells.** *Cell & bioscience* 2019, **9:**73.
24. Love MI, Huber W, Anders S: **Moderated estimation of fold change and dispersion for RNA-seq data with DESeq2.** *Genome Biol* 2014, **15:**550.
25. Jha P, Banda H, Tytarenko R, Bora PS, Bora NS: **Complement mediated apoptosis leads to the loss of retinal ganglion cells in animal model of glaucoma.** *Molecular immunology* 2011, **48:**2151-2158.
26. Fishelson Z, Attali G, Mevorach D: **Complement and apoptosis.** *Molecular immunology* 2001, **38:**207-219.
27. Murakami Y, Ishikawa K, Nakao S, Sonoda K-H: **Innate immune response in retinal homeostasis and inflammatory disorders.** *Progress in Retinal and Eye Research* 2019**:**100778.
28. Litvinchuk A, Wan Y-W, Swartzlander DB, Chen F, Cole A, Propson NE, Wang Q, Zhang B, Liu Z, Zheng H: **Complement C3aR Inactivation Attenuates Tau Pathology and Reverses an Immune Network Deregulated in Tauopathy Models and Alzheimer's Disease.** *Neuron* 2018, **100:**1337-1353.e1335.
29. Reichenbach N, Delekate A, Plescher M, Schmitt F, Krauss S, Blank N, Halle A, Petzold GC: **Inhibition of Stat3-mediated astrogliosis ameliorates pathology in an Alzheimer's disease model.** *EMBO molecular medicine* 2019, **11**.
30. Rosenfeld PJ, Brown DM, Heier JS, Boyer DS, Kaiser PK, Chung CY, Kim RY: **Ranibizumab for neovascular age-related macular degeneration.** *New England Journal of Medicine* 2006, **355:**1419-1431.
31. Kannan R, Hinton DR: **Sodium iodate induced retinal degeneration: new insights from an old model.** *Neural Regen Res* 2014, **9:**2044-2045.
32. Kiuchi K, Yoshizawa K, Shikata N, Moriguchi K, Tsubura A: **Morphologic characteristics of retinal degeneration induced by sodium iodate in mice.** *Curr Eye Res* 2002, **25:**373-379.
33. Moriguchi M, Nakamura S, Inoue Y, Nishinaka A, Nakamura M, Shimazawa M, Hara H: **Irreversible Photoreceptors and RPE Cells Damage by Intravenous Sodium Iodate in Mice Is Related to Macrophage Accumulation.** *Invest Ophthalmol Vis Sci* 2018, **59:**3476-3487.

34. Pujol-Lereis LM, Schafer N, Kuhn LB, Rohrer B, Pauly D: **Interrelation Between Oxidative Stress and Complement Activation in Models of Age-Related Macular Degeneration.** *Adv Exp Med Biol* 2016, **854:**87-93.
35. Lenis TL, Sarfare S, Jiang Z, Lloyd MB, Bok D, Radu RA: **Complement modulation in the retinal pigment epithelium rescues photoreceptor degeneration in a mouse model of Stargardt disease.** *Proceedings of the National Academy of Sciences of the United States of America* 2017, **114:**3987-3992.
36. Pauly D, Agarwal D, Dana N, Schafer N, Biber J, Wunderlich KA, Jabri Y, Straub T, Zhang NR, Gautam AK, et al: **Cell-Type-Specific Complement Expression in the Healthy and Diseased Retina.** *Cell Rep* 2019, **29:**2835-2848.e2834.

Figures

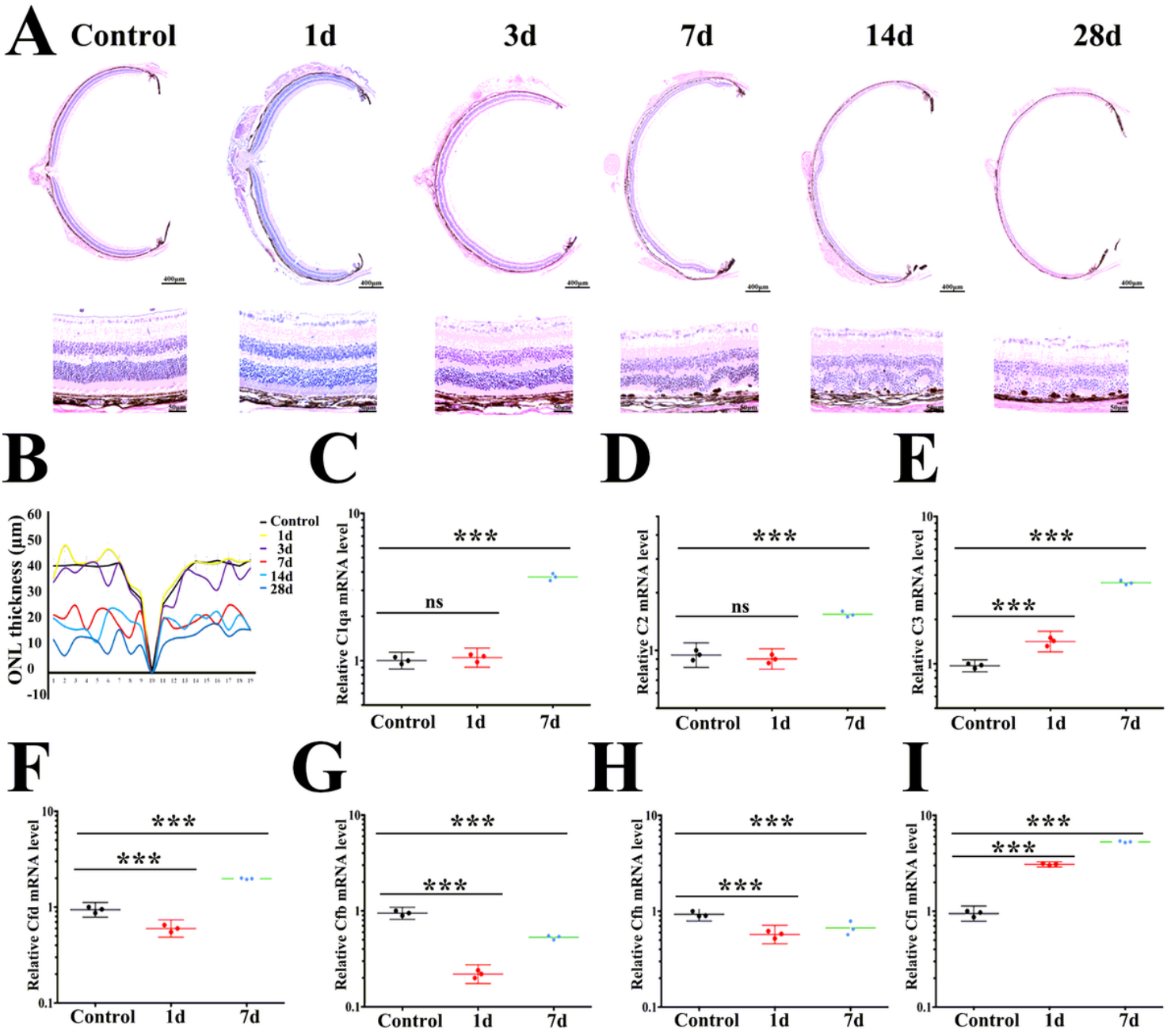

Figure 1

The complement system is activated in in NaIO3 mice model. A. HE staining of wild-type mice 0d to 28d after NaIO3 injection. B. ONL thickness of wild-type mice 0d to 7d after NaIO3 injection. C-I. Real-time PCR analysis of C1qa, C2, C3, Cfd, Cfb, Cfh and Cfi mRNA level in wild-type mice of 0d to 7d after NaIO3 injection. Data represent the mean+ SEM, n=3. *** p<0.001.

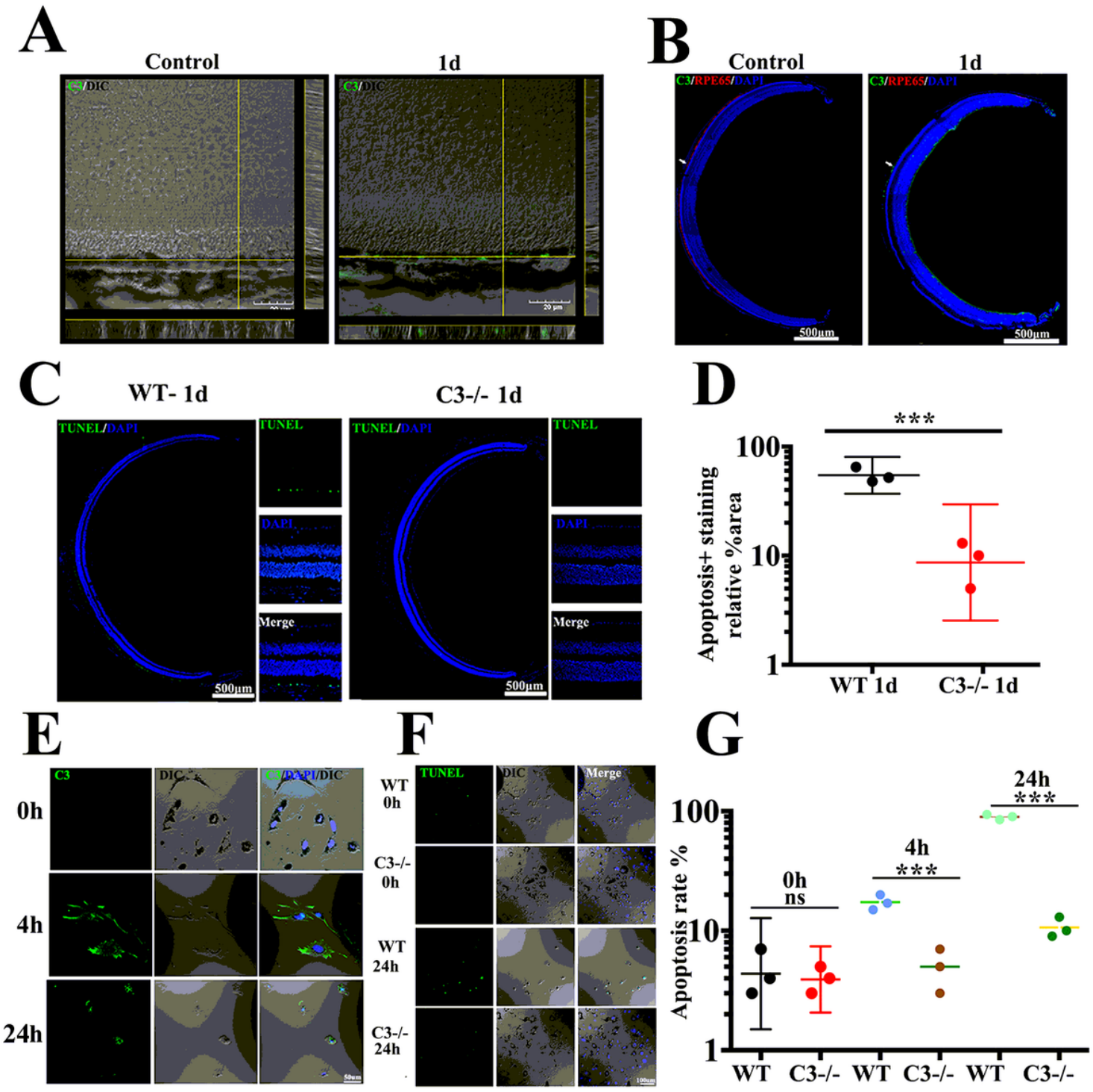

Figure 2

Intracellular C3 activation in RPE cells after NaIO3 induction in vivo and in vitro. A. Double immunofluorescent staining C3 (green) and RPE65 (red) of wild-type 0d and 1d after NaIO3 injection. B. Confocal assay of C3 localization of wild-type 0d and 1d after NaIO3 injection. C. TUNEL immunofluorescent staining of wild-type and C3-deficient mice 1d after NaIO3 injection. D. Quantification of (C). E. Immunofluorescent staining of C3 in RPE cells in vitro culture system at 0, 4, 24 hours after

NaIO3 induction. F. Immunofluorescent staining of TUNEL in RPE cells in vitro culture system at 0, 4, 24 hours after NaIO3 induction. G. Quantification of (F). Data represent the mean+ SEM, n=3. *** p<0.001.

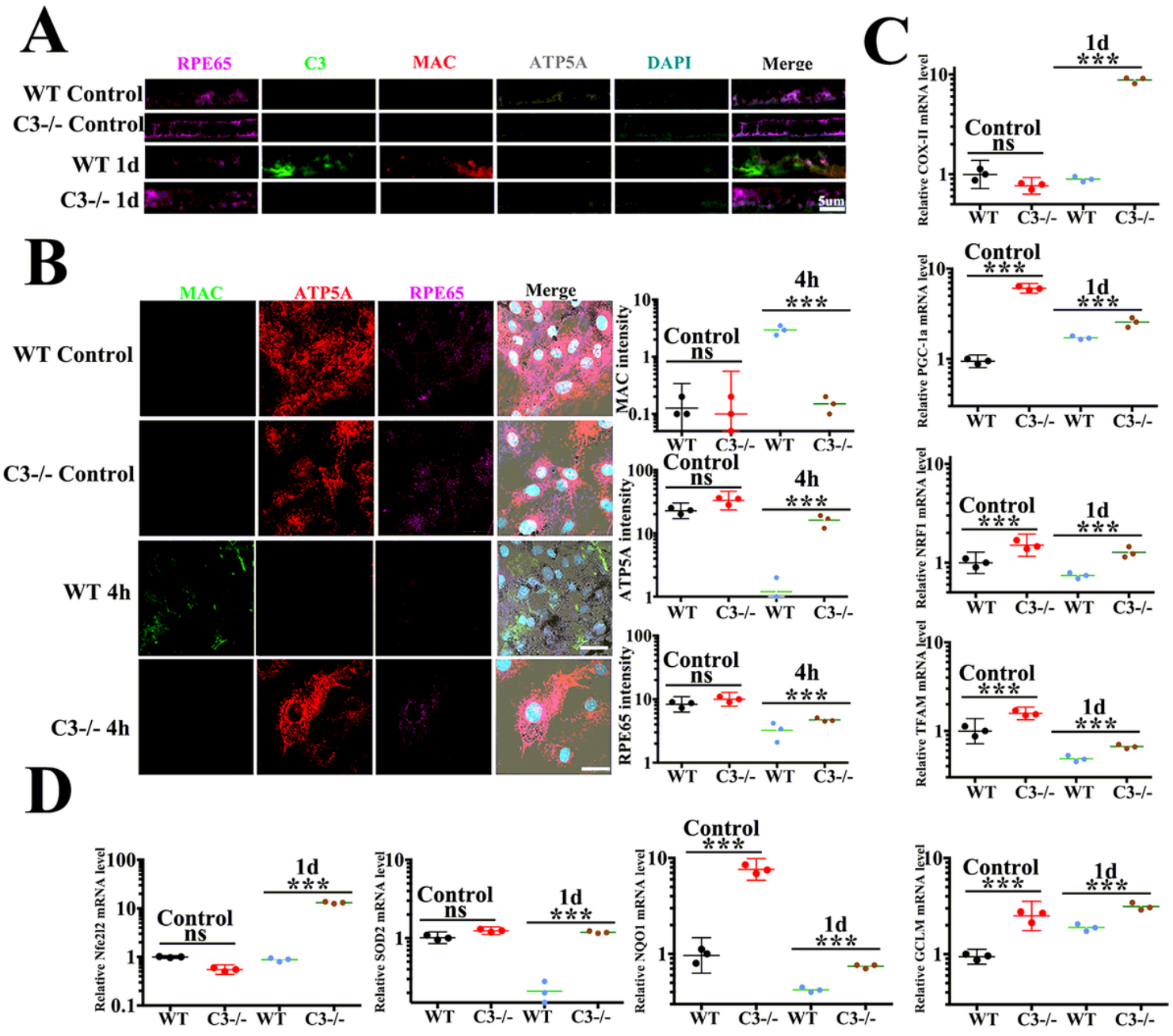

Figure 3

C3 activation-initiated MAC formation and mitochondrial malfunction in RPE cells after NaIO3 inducted oxidative stress in vivo and in vitro. A. Multicolor immunofluorescent staining of RPE65 (violet), C3 (green), MAC (red), ATP5A (gray) and DAPI (indigo) of wild-type and C3 knockout mice 1d after NaIO3 injection. B. Multicolor immunofluorescent staining and quantification of MAC (green), ATP5A (red), RPE65 (violet) and DAPI (indigo) in RPE cells in vitro culture system at 0 and 4 hours after NaIO3 induction. C. Real-time PCR analysis of COX-Ⅱ, PGC-1α, NRF1 and TFAM mRNA level in wild-type and C3 knockout mice 1d after NaIO3 injection. D. Real-time PCR analysis of Nre2l2, SOD2, NQO1 and GCLM

mRNA level in wild-type and C3 knockout mice 1d after NaIO3 injection. Data represent the mean+ SEM, n=3. *** p<0.001.

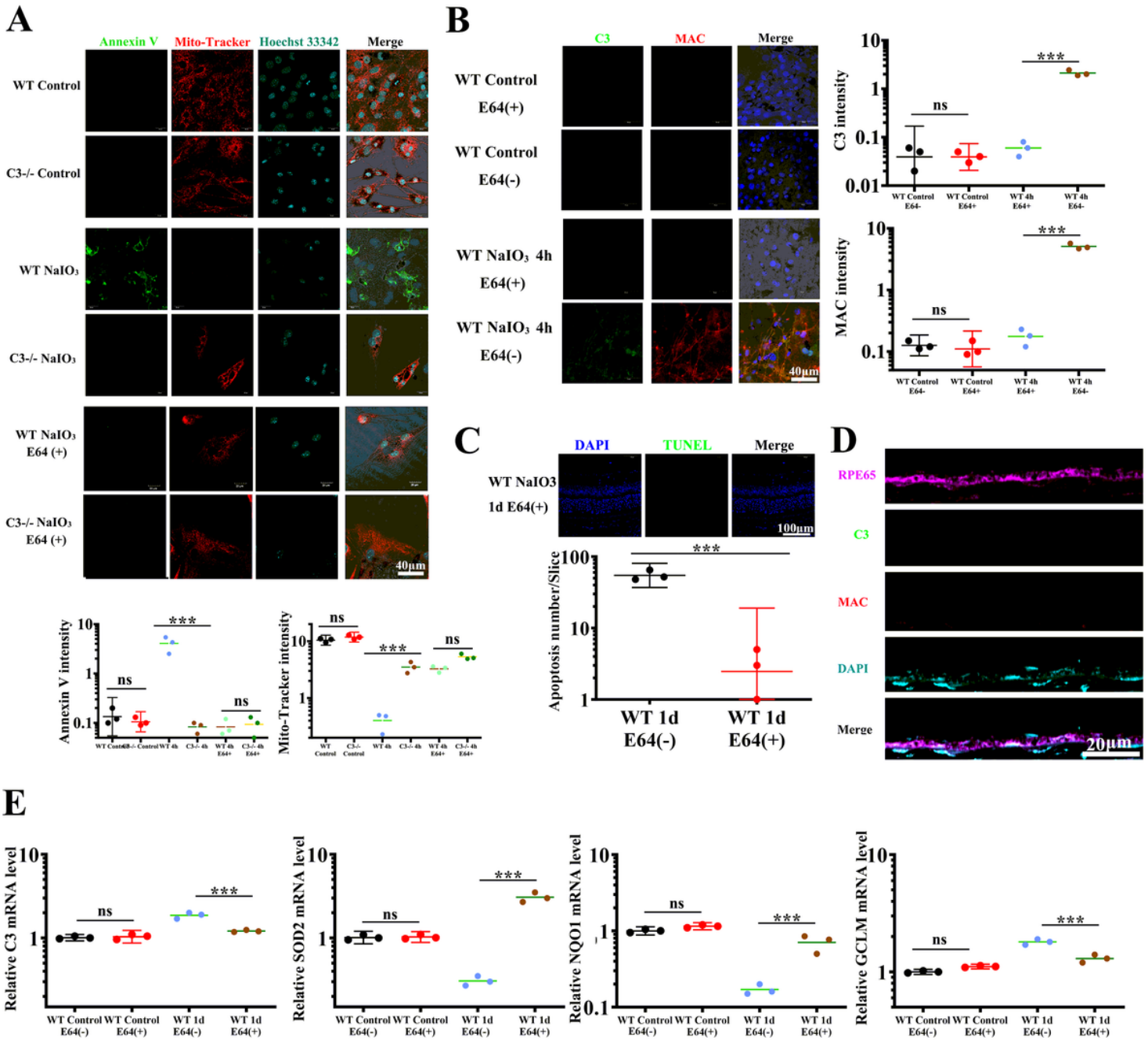

Figure 4

E64 attenuates intracellular C3 activation, apoptosis and mitochondrial malfunction of RPE cells after NaIO3 induction. A. Annexin V (green) and Mito-tracker (red) staining and confocal observation of wild-type and C3-deficient RPE cells after NaIO3 induction with or without E64 pre-treatment. B. Multicolor immunofluorescent staining of C3 (green), MAC (red) and DAPI (blue) of wild-type RPE cells after NaIO3 induction with or without E64 pre-treatment. C. Immunofluorescent staining and quantification of TUNEL

in retina at 1d after NaIO3 induction with E64 pre-treatment. D. Multicolor immunofluorescent staining of RPE65 (violet), C3 (green), MAC (red) and DAPI (indigo) of wild-type RPE cells after NaIO3 induction with E64 pre-treatment. E. Real-time PCR analysis of C3, SOD2, NQO1 and GCLM mRNA level in wild-type mice 0d and 1d after NaIO3 induction with or without E64 pre-treatment. Data represent the mean+ SEM, n=3. *** p<0.001.

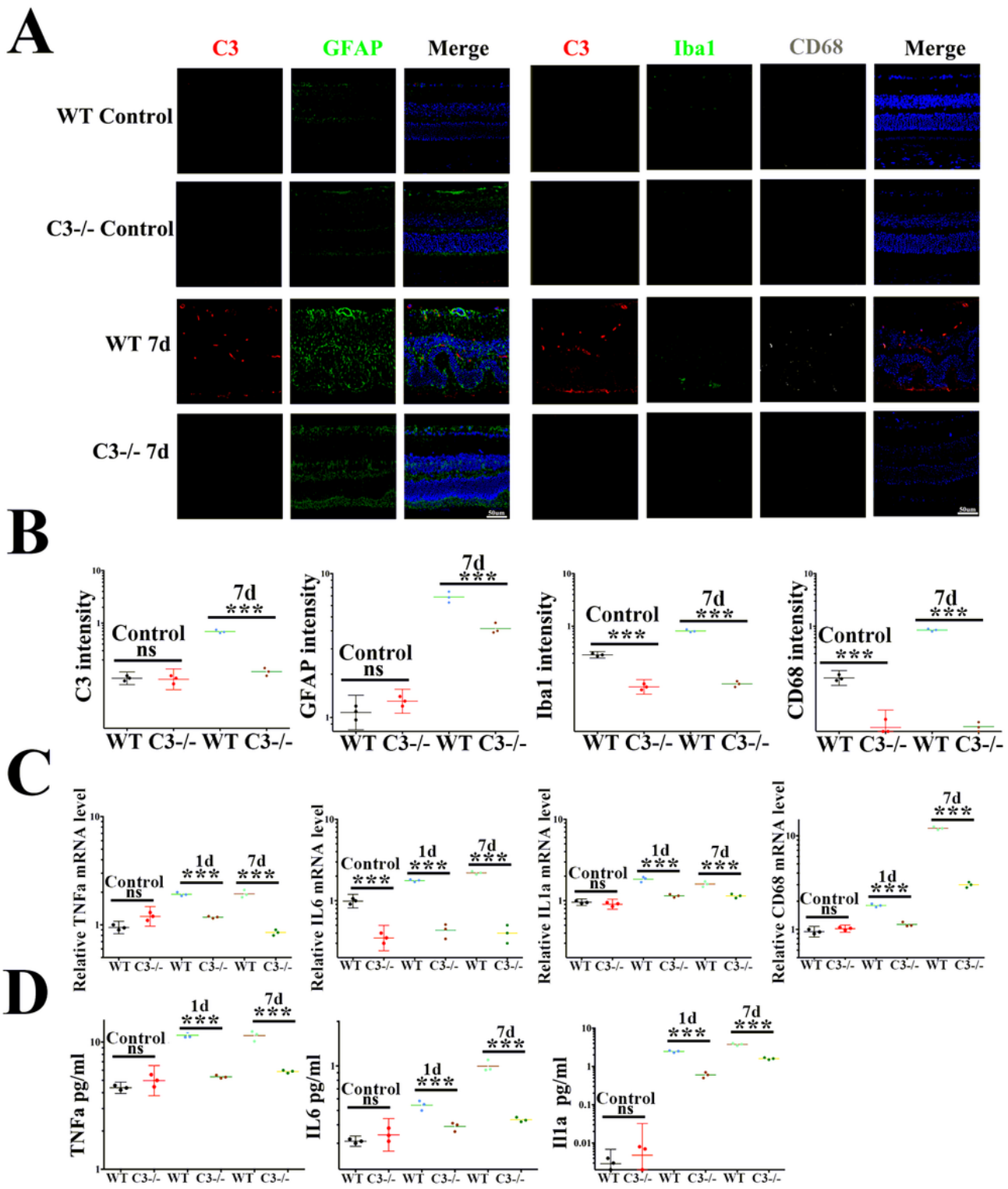

Figure 5

Genetic deletion of C3 attenuates reactive gliosis and microglia infiltration. A. Multicolor immunofluorescent staining and quantification of C3, GFAP, Iba1 and CD68 in retina of wild-type and C3-deficient mice 0d and 7d after NaIO3 injection. B. Quantification of C3, GFAP, Iba1 and CD68 immunoreactivities. C. Real-time PCR analysis of TNFα, IL6, IL1α and CD68 mRNA level in wild-type and C3-deficient mice 0d and 7d after NaIO3 induction. Data represent the mean+ SEM, n=3. *** p<0.001. D TNFα, IL6 and IL1α protein level in wild-type and C3-deficient mice measured by Elisa (mean+ SEM, n=3. *** p<0.001)

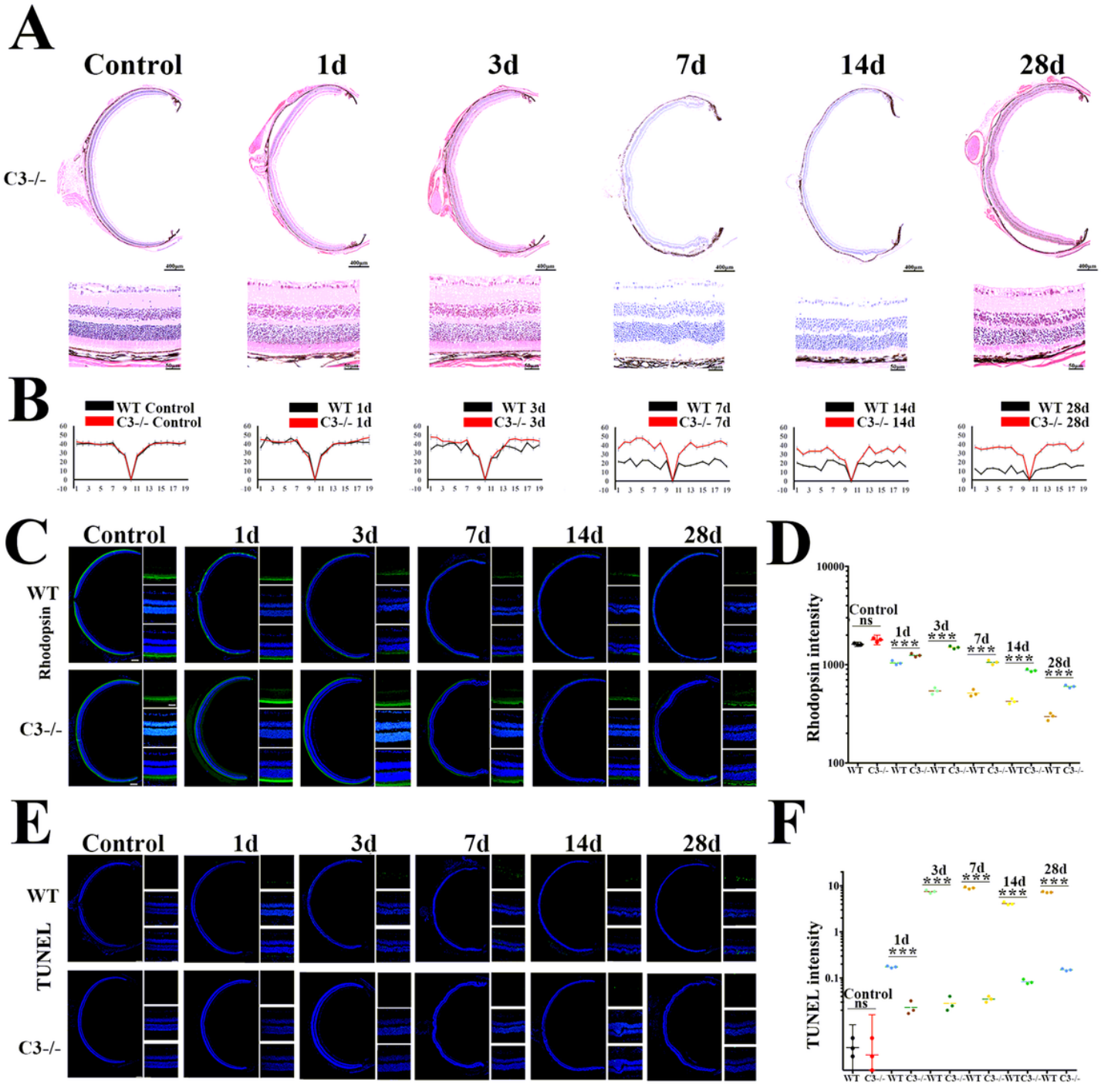

Figure 6

Knockout of C3 protect the neural retina structure in NaIO3 mice model. A. HE staining of C3-deficient mice 0d to 28d after NaIO3 injection. B. ONL thickness of wild-type and C3-deficient mice 0d to 28d after NaIO3 injection. C-F. Immunofluorescent staining and quantification of Rhodopsin and TUNEL in retina of wild-type and C3-deficient mice 0d to 28d after NaIO3 injection.

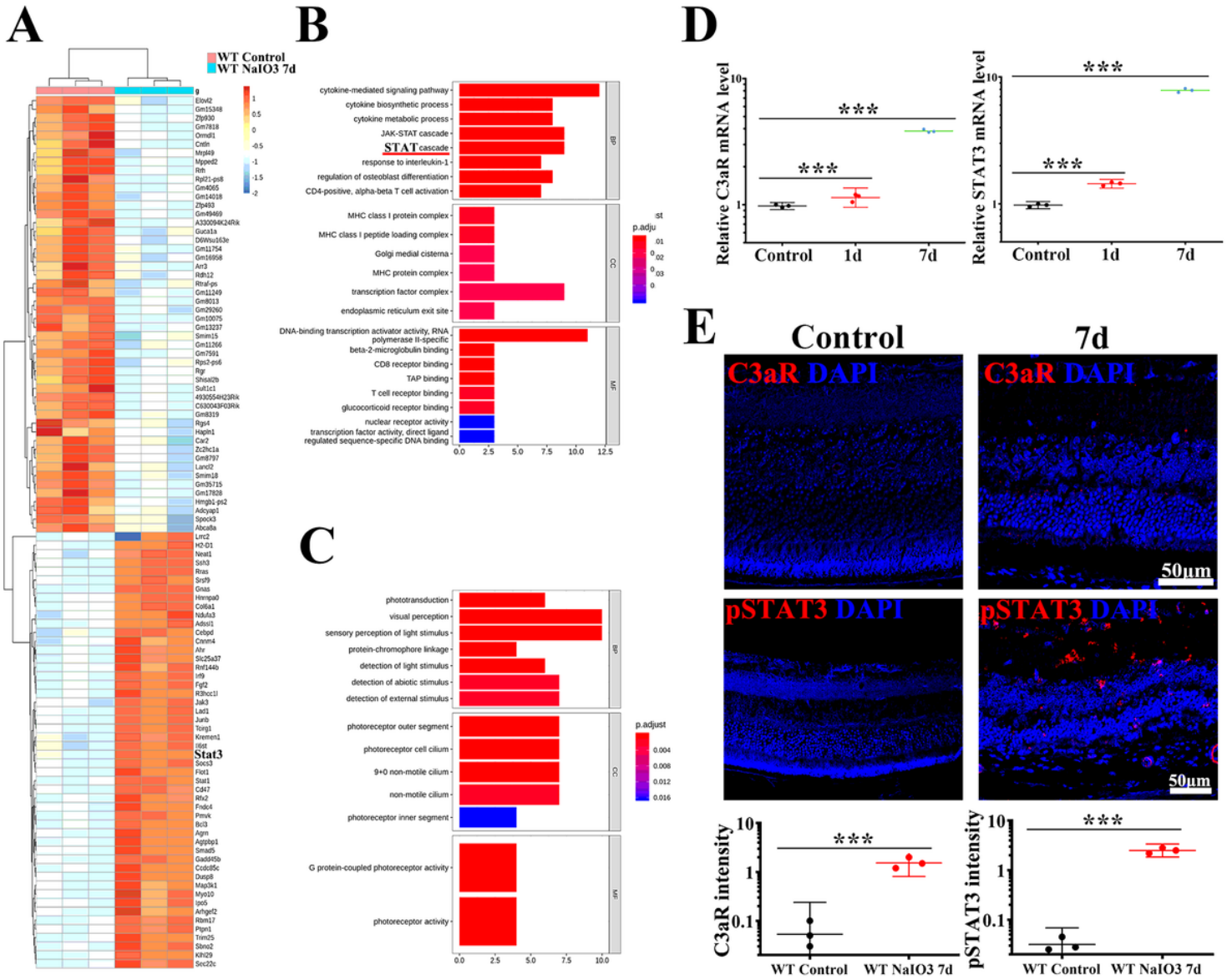

Figure 7

RNA-seq analysis identified C3/C3aR/STA3 signal pathway activation in NaIO3 mice model. A. DEGs identified top 100 changed gene in wild-type mice 0d and 7d after NaIO3 induction. B. Gene Ontology of up-regulated signal pathway. C. Gene Ontology of down-regulated signal pathway. D. Real-time PCR analysis of C3aR and STAT3 mRNA level in wild-type 0d, 1d and 7d after NaIO3 induction. Data represent the mean+ SEM, n=3. *** p<0.001. E. Immunostaining and quantification of C3aR and pSTAT3 in wild-type 0d and 7d after NaIO3 induction. Data represent the mean+ SEM, n=3. *** p<0.001.

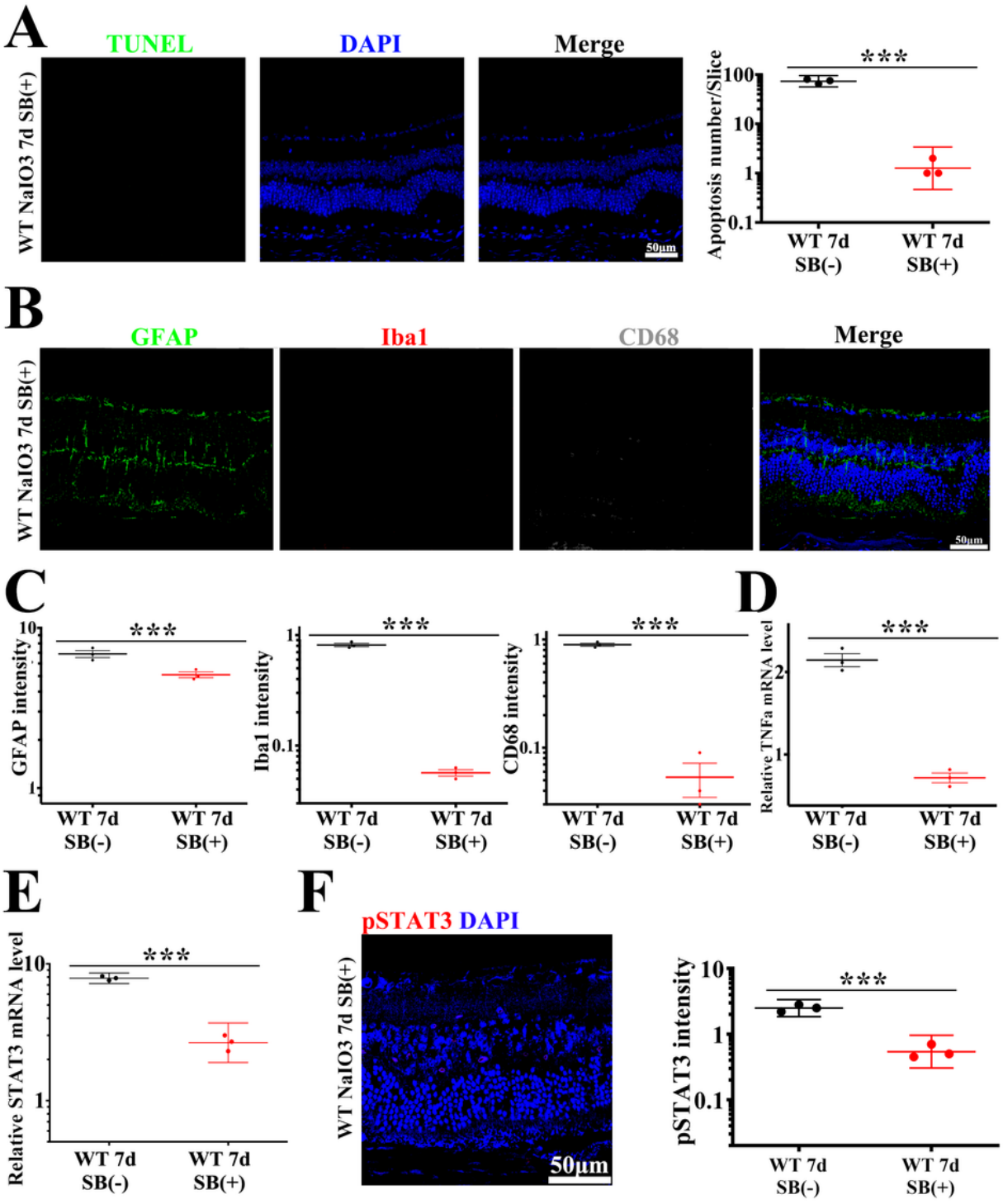

Figure 8

C3aR inhibitor reduced gliosis and microglial activation in NaIO3 mice model. A. Immunostaining of TUNEL in wild-type mice 7d after NaIO3 induction with SB290157 (SB) pretreatment. B, C. Multicolor immunofluorescent staining and quantification of GFAP, Iba1 and CD68 in wild-type mice 7d after NaIO3 induction with SB pretreatment. D, E. Real-time PCR analysis of TNFα and STAT3 mRNA level in wild-type

mice 7d after NaIO3 induction with SB pretreatment. F. Immunostaining of Pstat3 and quantification in wild-type mice 7d after NaIO3 induction with SB pretreatment.

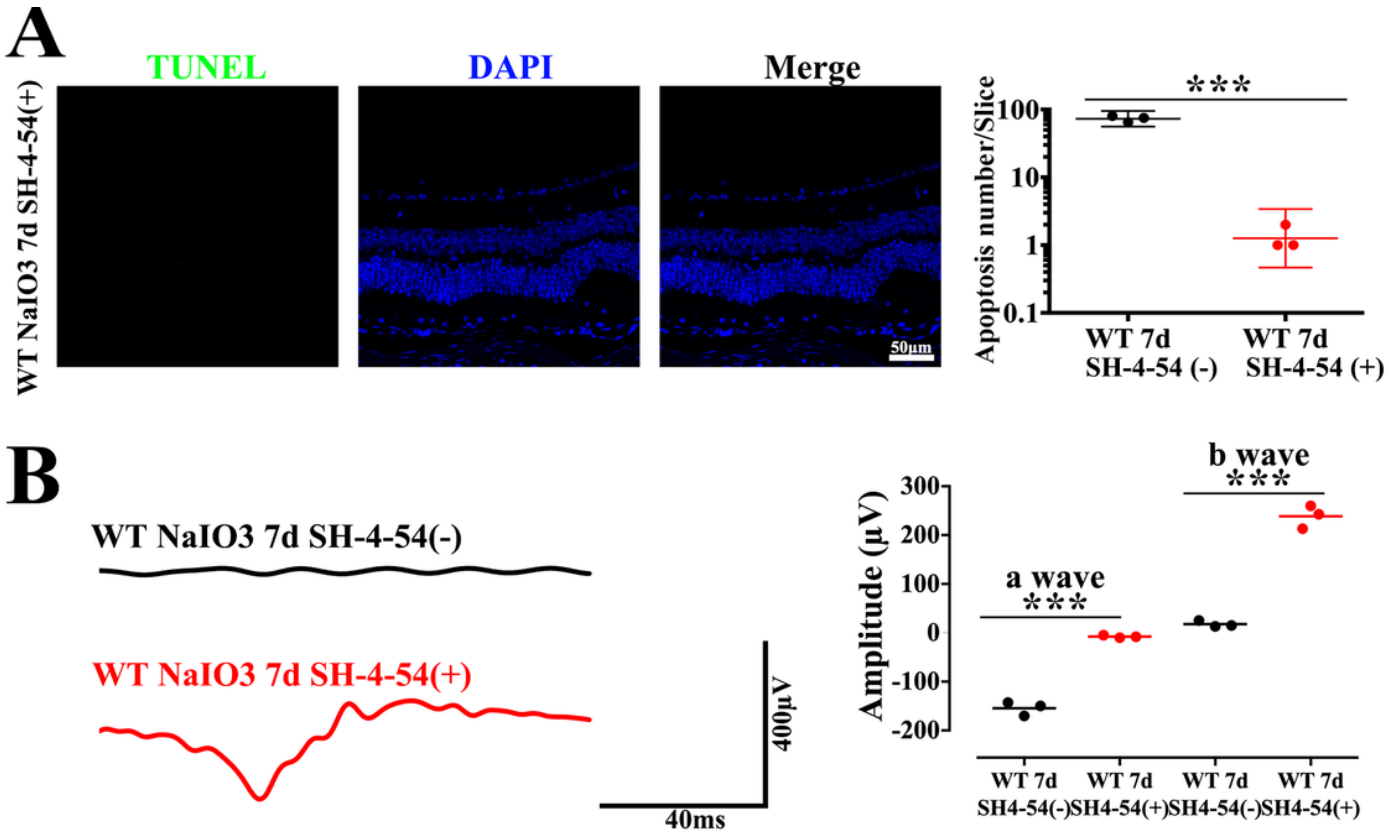

Figure 9

STAT3 inhibitor partial rescued retinal function of wild-type mice after NaIO3 induction. A. Immunostaining and quantification of TUNEL in wild-type mice 7d after NaIO3 induction with or without SH-4-54 pretreatment. B. ERG analysis of retinal function in wild-type mice 7d after NaIO3 induction with or without SH-4-54 pretreatment.

Supplementary Files

This is a list of supplementary files associated with this preprint. Click to download.

- FigureS1.tif
- FigureS2.tif